Journal of Cerebral Blood Flow & Metabolism (2012) 32, 874–883

www.jcbfm.com

Combining PET biodistribution and equilibrium dialysis assays to assess the free brain concentration and BBB transport of CNS drugs

Roger N Gunn[1,2,3], Scott G Summerfield[4], Cristian A Salinas[1], Kevin D Read[5], Qi Guo[1,3], Graham E Searle[1], Christine A Parker[1,3], Phil Jeffrey[6] and Marc Laruelle[3,7]

[1]*GlaxoSmithKline, Clinical Imaging Centre, Hammersmith Hospital, London, UK;* [2]*Department of Engineering Science, University of Oxford, Oxford, UK;* [3]*Department of Medicine, Imperial College, London, UK;* [4]*GlaxoSmithKline, DMPK, Ware, UK;* [5]*Division of Biological Chemistry and Drug Discovery, College of Life Sciences, University of Dundee, Dundee, UK;* [6]*GlaxoSmithKline, Epinova, DPU, Stevenage, UK;* [7]*GlaxoSmithKline, Neurosciences Centre of Excellence for Drug Discovery, Harlow, UK*

The passage of drugs in and out of the brain is controlled by the blood–brain barrier (BBB), typically, using either passive diffusion across a concentration gradient or active transport via a protein carrier. *In-vitro* and preclinical measurements of BBB penetration do not always accurately predict the *in-vivo* situation in humans. Thus, the ability to assay the concentration of novel drug candidates in the human brain *in vivo* provides valuable information for derisking of candidate molecules early in drug development. Here, positron emission tomography (PET) measurements are combined with *in-vitro* equilibrium dialysis assays to enable assessment of transport and estimation of the free brain concentration *in vivo*. The PET and equilibrium dialysis data were obtained for 36 compounds in the pig. Predicted P-glycoprotein (P-gp) status of the compounds was consistent with the PET/equilibrium dialysis results. In particular, Loperamide, a well-known P-gp substrate, exhibited a significant concentration gradient consistent with active efflux and after inhibition of the P-gp process the gradient was removed. The ability to measure the free brain concentration and assess transport of novel compounds in the human brain with combined PET and equilibrium dialysis assays can be a useful tool in central nervous system (CNS) drug development.
Journal of Cerebral Blood Flow & Metabolism (2012) **32,** 874–883; doi:10.1038/jcbfm.2012.1; published online 25 January 2012

Keywords: active transport; blood–brain barrier; equilibrium dialysis; passive diffusion; PET

Introduction

The discovery and development of central nervous system (CNS) drugs is a complex task that requires large investments of time and money with no guarantee of success. Therefore, increasing confidence in molecules early in development by derisking their chance of failure later on is of great value. For example, a key development question for CNS drugs is whether they can penetrate the blood–brain barrier (BBB) and reach the brain in pharmacologically active concentrations. Imaging techniques, such as positron emission tomography (PET), can provide important information by taking direct biological measurements in tissues of interest in preclinical and clinical species *in vivo*. Radiolabelling of a drug candidate with a positron emitter does not change the properties of the drug and subsequent injection of this radiolabelled drug into a subject allows for a biodistribution experiment, which measures the concentration of drug in tissues of interest. In the CNS after appropriate biomathematical correction for the contribution of radioactivity emanating from the blood vessels, it is possible to directly measure the total concentration of radiolabelled drug that reaches the brain tissue itself (Cunningham *et al*, 2005).

Previous applications of PET biodistribution experiments have effectively been performed in the context of a binary readout, i.e., does the drug get into the brain or not. However, the actual process is more complex and concentration gradients can exist across the BBB at equilibrium. The BBB controls passage of drugs in and out of the brain, typically, using either passive diffusion across a concentration gradient or active transport via a protein carrier.

Correspondence: Dr RN Gunn, Imanova Limited, Imperial College London, Hammersmith Hospital, Burlington Danes Building, Du Cane Road, London W12 0NN, UK.
E-mail: roger.gunn@imanova.co.uk
This study was funded by GlaxoSmithKline.
Received 22 July 2011; revised 8 November 2011; accepted 16 December 2011; published online 25 January 2012

Under the process of passive diffusion, the concentration of free drug in plasma and tissue will be equal at equilibrium. However, if there are active transport mechanisms involved there will be a concentration gradient established between plasma and tissue with the magnitude of the gradient depending on the active transport system involved and the properties of the drug molecule itself. These transporters tend to act to remove drugs from the brain and this process is known as BBB carrier-mediated efflux, with the ABC (ATP) binding cassette transporters, P-glycoprotein (P-gp), and the multidrug resistance-associated proteins being the most characterized to date (Cordon-Cardo *et al*, 1989; Borst and Oude Elferink 2002; Giacomini *et al*, 2010).

A key goal in drug development is to measure the free concentration in the brain tissue, as in conjunction with other *in-vitro*/preclincial data it allows for an assessment of whether the drug achieves a pharmacologically active concentration in the brain (Hammarlund-Udenaes *et al*, 2008, 2009). Thus, it is the assay of the free brain concentration and assessment of any active transport liabilities that provide the most valuable information for derisking the compound early in development. These studies can be performed in relevant preclinical species and if performed in humans should be combined as part of a first time in human study to maximize their value.

To assay the free concentration in the brain tissue (not just the total concentration), it is necessary to account for the nonspecific component of the signal in tissue from binding to lipids and in plasma from binding to plasma proteins. This information is not independently available from the PET data itself and requires a complementary assay of the plasma- and tissue-free fractions (f_P and f_{ND}, respectively). f_P can be assayed in conjunction with PET experiments by applying ultrafiltration techniques to the radiolabelled compound in a plasma sample (Gandelman *et al*, 1994). However, ultrafiltration estimates can be poor when f_P is small and it is not possible to estimate f_{ND} with this approach. Here, we propose the use of equilibrium dialysis (Kalvass and Maurer 2002; Summerfield *et al*, 2006) to measure the nonspecific binding components of the unlabelled drug candidates in both plasma and tissue. Equilibrium dialysis allows for the measurement of free drug fractions in brain tissue (f_{ND}) and plasma (f_P) and has been used in drug development as an *in-vitro* screen for BBB penetration by considering the ratio (f_P/f_{ND}) as a predictor of the brain to blood partition coefficient under the assumption of passive diffusion (Summerfield *et al*, 2006; Jeffrey and Summerfield, 2007). In addition, under the assumption of passive diffusion and the existence of target affinity estimates, predictions of target occupancy can be made (Read and Braggio, 2010).

The work presented here aims to combine *in-vivo* PET measurements of a radiolabelled drug with *in-vitro* equilibrium dialysis assays to estimate the free brain concentration of the drug and assess its transport process. These principles were investigated using a set of 36 compounds and the Yorkshire-Landrace pig. All compounds were radiolabelled and quantitative dynamic PET experiments were performed with each compound to derive the nondisplaceable partition coefficient (V_{ND}). In addition, each compound was analyzed with equilibrium dialysis in pig blood and brain tissue to derive estimates of f_P and f_{ND}. Finally, each compound underwent an *in-silico* analysis to predict its P-gp status.

Materials and methods

The free concentration of a compound in tissue and plasma can be defined as

$$\begin{aligned} C_{FP} &= f_P C_P \\ C_{FT} &= f_{ND} C_{ND} \end{aligned} \tag{1}$$

where C_P is the total plasma concentration, C_{ND} is the total tissue concentration of the nondisplaceable component, C_{FP} and C_{FT} are the free concentrations in plasma and tissue, respectively, f_P and f_{ND} are the plasma- and tissue-free fractions, respectively. Using these equations and the definition of the equilibrium partition coefficient, V_{ND}, which equals the ratio of total tissue and total plasma concentration at equilibrium,

$$V_{ND} = \frac{C_{ND}}{C_P} \tag{2}$$

gives,

$$V_{ND} = \frac{f_P}{f_{ND}} \frac{C_{FT}}{C_{FP}} \tag{3}$$

Thus, the equilibrium partition coefficient is defined as the product of two ratios, the first (f_P/f_{ND}) is determined by nonspecific binding properties and the second (C_{FT}/C_{FP}) is determined by BBB properties. If it is assumed that the compound crosses the BBB by passive diffusion, then the free concentration in plasma and tissue at equilibrium will be equal and equation (3) reduces to the common form

$$V_{ND} = \frac{f_P}{f_{ND}} \tag{4}$$

This equation is frequently used in conjunction with f_P from ultrafiltration and V_{ND} from PET to derive an estimate of f_{ND} and subsequently correct binding outcome measures for nuisance nonspecific binding terms (Innis *et al*, 2007). However, it is important to remember that such corrections are only valid if the radioligand crosses the BBB by passive diffusion.

Alternatively, if no assumption about transport mechanisms is made and separate estimates of the free fractions in plasma and tissue are available, then it is possible to determine the free concentration in tissue (C_{FT}) or the concentration gradient at the BBB (C_{FT}/C_{FP}).

To investigate this, a set of 36 compounds that had been previously radiolabelled and used in quantitative dynamic PET studies in the Yorkshire-Landrace pig was used. All compounds underwent *in-vitro* equilibrium dialysis assays

in pig plasma and tissue to estimate their free fractions (f_P and f_{ND}). P-glycoprotein was assumed to be the only active transport mechanism and a compound's P-gp status was either determined from separate experimental data or via *in-silico* modelling technique.

In-Silico P-Glycoprotein Assay

A proprietary categorical model was used to determine P-gp status (e.g., substrate or nonsubstrate) based on Partial least squares-Discriminant analysis. Model development used a training set of 100 P-gp substrates and 100 P-gp nonsubstrates, a test set of 454 compounds (116 substrates and 338 nonsubstrates), a validation set with 415 compounds (118 substrates and 297 nonsubstrates) measured at different concentrations (from 0.5 to 3 μmol/L) and a second validation set with 574 compounds (216 substrates and 358 nonsubstrates) measured at different concentrations (from 5 to 20 μmol/L). Coefficients were found to be negative for the Abraham Alpha and BetaH terms and total charge, and positive for ACD $cLogD_{7.4}$ and ACD clogP. A positive value signifies the molecule will be classified as P-gp substrate. Distance from the discriminant line was used as a confidence indicator in the derived classification (P-gp score).

In-Vitro Equilibrium Dialysis Assay

The equilibrium dialysis methodology followed for this work has been described previously (Summerfield *et al*, 2006). Briefly, test compounds were spiked into control blood, plasma, or brain homogenate at a concentration of 1 μg/g and dialyzed against PBS (pH 7.4) for 5 hours at 37°C. Aliquots (20 to 50 μL) of plasma, blood, brain, and dialysate were taken and extracted using acetonitrile containing internal standard, followed by LC-MS/MS analysis. Landrace pig plasma and fresh brain tissue were obtained from Charles River Laboratories (Tranent, Scotland). The unbound fractions were determined as the concentration ratio of analyte in dialysate to that in plasma or brain. Note: These data were obtained from different animals than those that underwent the PET scans.

In-Vivo Positron Emission Tomography Assay

All compounds ($n = 36$, see Table 1) were radiolabelled with either C-11 or F-18 and evaluated in PET studies in the Yorkshire/Danish Landrace pig (~40 kg), at Aarhus University Hospital, in accordance with the Danish Animal Experimentation Act, under a license granted by the Danish Ministry of Justice. The animals were anesthetized by induction with ketamine and midazolam (both intramuscular and intravenous) during scans and maintained in deep anesthesia using isofluorane (1% to 2%; Abbott, Copenhagen, Denmark). Animals were placed supine in a Siemens ECAT EXACT HR tomograph (CTI, Knoxville, TN, USA), with the head immobilized in a custom-made head-holding device. Dynamic data were acquired in 3D mode positioned over the brain, for a duration of between 60 and 90 minutes, after intravenous administration of the radiolabelled compound (injected radioactivity: 318.0 ± 127.5 MBq, range (100 to 517 MBq)). Some scans, for tracers whose target was expressed in the cerebellum, included the addition of homologous or heterologous agents to block any specific binding component (details of the blocking agents and doses are given in Table 1). With [^{11}C]Loperamide two scans were performed, one in the absence and one in the presence of cyclosporin-A (30 mg), a known P-gp inhibitor (Qadir *et al*, 2005). Measured attenuation correction and scatter correction were applied and the data were reconstructed using the reprojection algorithm (Kinahan and Rogers, 1989) with an axial and transaxial Hanning filter with a 0.5 cutoff frequency. The resulting images had a spatial resolution of 5 to 7 mm full width at half maximum (Wienhard *et al*, 1994). During the acquisition, up to 40×2 mL arterial blood samples were taken from the femoral artery to assay radioactivity in arterial plasma; in addition, a subset of up to 17 were assayed for whole blood radioactivity. Total radioactivity in arterial plasma and whole blood was measured using a gamma counter (Cobra II Auto Gamma, Packard, Meriden, CT, USA). Additional arterial samples (up to 6×5 mL) were drawn through the scan to determine the fraction of unmetabolized tracer in plasma by high-performance liquid chromatography and gamma counting. Integrated PET images were formed and used to rigidly register the PET data to a Landrace pig brain atlas. Cerebellar time activity curves (TACs) were generated for each radiolabelled compound. The cerebellum was chosen as the region of interest for two reasons. First, it is often devoid of the receptors and transporters relevant for a large number of the radioligands considered here. Second, it is a good sized region, which provides strong imaging statistics and reduces errors associated with the PET outcome measures of interest.

Parent plasma input functions, $C_p(t)$, were generated for each scan by interpolating the discrete plasma data using linear interpolation, and multiplying this by the continuous parent fraction derived from fitting the discrete metabolite data to an appropriate model. The parent fraction model was selected on the basis of goodness of fit from a family of possible models. The models considered were

Model A: Exponential approach to a constant

$$P_F(t) = (1-\alpha)e^{-\beta t} + \alpha \quad (5)$$

Model B: Single exponential

$$P_F(t) = e^{-\beta t} \quad (6)$$

Model C: Two exponential with constrained washout

$$P_F(t) = (1-\alpha)e^{-\beta t} + \alpha e^{-\gamma t} \quad (7)$$

where γ is constrained to equal the difference between (γ_{CER}) the terminal rate of washout of the nondisplaceable cerebellar TAC and (γ_P) the smallest elimination rate constant of the total plasma ($\gamma = \gamma_{CER} - \gamma_P$; Abi-Dargham *et al*, 1999).

Table 1 Summary of the *in-silico*, *in-vitro,* and *in-vivo* data for the ($n = 36$) compounds studied

Compound name	In-silico *modelling P-gp score*	*Equilibrium dialysis*			*PET*						
		f_P	f_{ND}	f_P/f_{ND}	*Parent fraction*	*ROI*	*Blocking agent*	*Blocking dose*	*Kinetic analysis*	K_1	V_{ND}
SB-611000[a]	−3.46	0.0668	0.0092	7.27	Model A	Cerebellum			Model II	0.07	2.74
SB-611093-AY[a]	−1.26	0.1378	0.0104	13.22	Model C	Cerebellum			Model I	0.06	2.34
GSK200742[a]	−1.02	0.2679	0.0402	6.66	Model A	Cerebellum			Model I	0.01	0.81
NMSP	−0.77	0.1584	0.0483	3.28	Model A	Cerebellum[b]	S(−)sulpiride	25.0000	Model II	0.32	3.6
GSK224558	−0.63	0.1234	0.0135	9.14	Model B	Cerebellum[b]	GSK224558	0.5000	Model I	0.8	9.66
Loperamide[a]	−0.62	0.1793	0.013	13.83	Model A	Cerebellum			Model I	0.05	4.6
GW876008	−0.56	0.0356	0.012	2.97	Model A	Cerebellum[b]	GW808990	10.0000	Model II	0.55	5.07
GW692155	−0.53	0.0103	0.001	10.77	Model A	Cerebellum			Model II	0.07	2.48
GSK189254	−0.51	0.4646	0.3836	1.21	Model A	Cerebellum[b]	GSK189254	0.0500	Model II	0.46	2.46
GSK215083	−0.43	0.288	0.0394	7.31	Model A	Cerebellum[b]	GSK215083	0.0050	Model II	0.62	7.59
SB-587828-A[a]	−0.4	0.0822	0.0107	7.68	Model A	Cerebellum			Model I	0.04	1.67
GR205171	−0.27	0.299	0.0646	4.63	Model A	Cerebellum[b]	GR205171	0.0625	Model II	0.49	7.68
FLB-457	−0.21	0.4758	0.2114	2.25	Model A	Cerebellum			Model II	0.55	3.2
MDL 100907	−0.19	0.4753	0.1201	3.96	Model A	Cerebellum			Model I	0.56	7.99
GW775236[a]	−0.03	0.0257	0.0011	22.69	Model A	Cerebellum[b]	GR205171	0.0625	Model II	0.24	12.15
GSK991022A	0.03	0.0092	0.101	0.09	Model A	Cerebellum[b]	GSK565710	0.5000	Model II	0.03	0.79
Flumazenil	0.09	0.6295	0.5531	1.14	Model A	Cerebellum			Model II	0.49	1.24
GW700382	0.1	0.0728	0.0029	24.83	Model B	Cerebellum[b]	GR205171	0.0625	Model II	0.47	29.69
GSK219920	0.11	0.0271	0.0109	2.49	Model A	Cerebellum			Model II	0.01	0.23
GW194712	0.11	0.0133	0.0018	7.42	Model A	Cerebellum[b]	GR205171	0.0625	Model II	0.47	8.34
GW406381	0.21	0.0723	0.0107	6.75	Model A	Cerebellum			Model II	0.58	5.44
GSK981352	0.23	0.327	0.147	2.22	Model C	Cerebellum[b]	SB-277011	0.5000	Model II	0.61	3.26
GW223994[a]	0.27	0.124	0.0094	13.21	Model A	Cerebellum[b]	GR205171	0.0625	Model II	0.37	8.15
GSK931145	0.36	0.2786	0.0997	2.79	Model A	Cerebellum[b]	GSK931145	0.0500	Model II	0.12	1.12
GW679982A	0.36	0.059	0.0098	6	Model A	Cerebellum			Model II	0.22	6.77
GW685944	0.36	0.0129	0.0014	9.21	Model A	Cerebellum			Model I	0.2	9.49
GW782682	0.37	0.0036	0.0008	4.69	Model B	Cerebellum			Model I	0.13	3.48
GSK1018921	0.48	0.0245	0.0415	0.59	Model A	Cerebellum[b]	GSK565710	0.5000	Model II	0.08	1
Raclopride	0.54	0.1509	0.1343	1.12	Model A	Cerebellum			Model II	0.33	1.11
GSK565710	0.56	0.129	0.0161	8.01	Model A	Cerebellum[b]	GSK565710	0.5000	Model II	0.22	5.4
GSK819555	0.58	0.0012	0.0007	1.73	Model A	Cerebellum			Model II	0.16	5.11
R-(+)-rolipram	0.59	0.2577	0.1922	1.34	Model A	Cerebellum[b]	R(−)Rolipram	0.0100	Model II	0.61	3.47
S-(+)-rolipram	0.59	0.3002	0.1936	1.55	Model A	Cerebellum[b]	S(+)Rolipram	0.2500	Model II	0.28	2.63
GW644784	0.71	0.0236	0.0038	6.22	Model A	Cerebellum			Model II	0.27	10.11
GSK574734	0.77	0.3185	0.2301	1.38	Model A	Cerebellum			Model II	0.22	0.38
PK11195	1.02	0.0658	0.0226	2.9	Model A	Cerebellum[b]	PK11195	5.0000	Model II	0.35	4.87

P-gp, P-glycoprotein; ROI, region of interest; PET, positron emission tomography.

The *in-silico* P-gp score is a metric from a computer model that indicates whether the compound is likely to be a P-gp substrate—negative numbers indicate that the compound is likely to be a substrate with increasingly negative numbers imparting an increased confidence. *In-vitro* equilibrium dialysis data give the plasma (f_P) and tissue (f_{ND}) free fraction from plasma and brain homogenate, respectively. For the analysis of the *in-vivo* PET data, the choice of parent fraction and kinetic analysis method are detailed along with the estimated plasma clearance (K_1—mL/min/cm^3) and equilibrium partition coefficient (V_{ND}—mL/cm^3) for cerebellum. Model A—Exponential approach to a constant, Model B—Single exponential, Model C—Two exponential with constrained washout, Model I—One-tissue compartmental analysis, and Model II—Two-tissue compartmental analysis.

[a]Compounds identified from analysis of the *in-vitro–in-vivo* data to be P-gp substrates by *post hoc* Z-tests (see text).

[b]Cerebellum data were obtained from a scan after preadministration of a compound to block specific binding with an associated blocking agent (doses are given in mg/kg).

A whole blood input function, $C_B(t)$, was also generated and used to correct the cerebellar TAC for vascular radioactivity. Cerebellar V_{ND} estimates were obtained from kinetic analysis using either a one-tissue (Model I) or two-tissue (Model II) compartmental model according to

$$C_T(t) = V_B C_B(t) + (1 - V_B)\mathrm{IRF}(t) \otimes C_p(t) \quad (8)$$

where IRF(t) is the impulse response function and V_B is the fractional blood volume. The impulse response function for the one-tissue model is given by

$$\mathrm{IRF}(t) = \phi_1 e^{-\theta_1 t} \quad (9)$$

and for the two-tissue model it is given by

$$\mathrm{IRF}(t) = \phi_1 e^{-\theta_1 t} + \phi_2 e^{-\theta_2 t} \quad (10)$$

The V_{ND} is obtained from the impulse response function as

$$V_{ND} = \int_0^\infty \mathrm{IRF}(t)\,dt \quad (11)$$

and the plasma clearance rate constant (K_1) as

$$K_1 = \sum_i \phi_i \quad (12)$$

The least squares fitting procedure included a fixed 5% blood volume and was performed with a Levenberg–Marquadt optimiser in the Matlab software environment (Matlab, Natwick, MA, USA). The Akaike information criterion was used as the model selection criteria to determine the most parsimonious kinetic model.

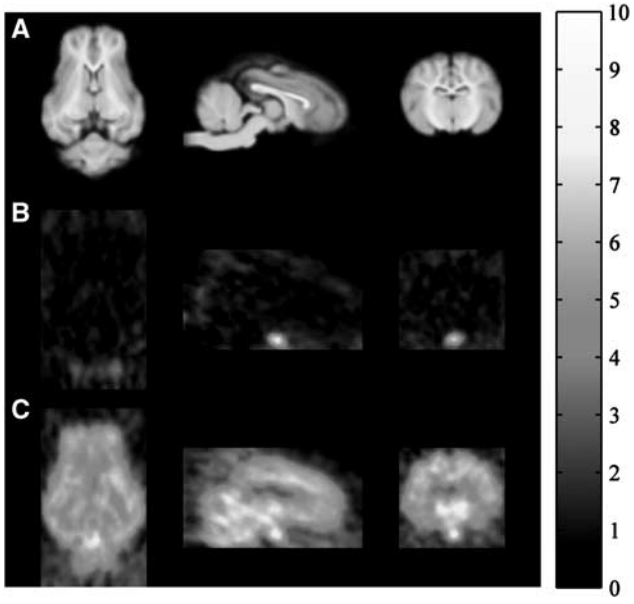

Figure 1 Magnetic resonance imaging (MRI) (**A**) and positron emission tomography (PET) (**B**, **C**) images of the Yorkshire-Landrace Pig brain in transaxial, sagittal, and coronal sections (MRI and PET data are obtained from different animals). (**A**) Structural T1-weighted MRI scans for anatomical reference. (**B**, **C**) [^{11}C]Loperamide PET scans (integral images 0 to 90 minutes) displayed in standardized uptake units (%ID/L); panel **B** is at baseline and indicates very little uptake for the known P-glycoprotein (P-gp) substrate, whereas panel **C** is after administration of cyclosporin-A (30 mg) which inhibits the P-gp efflux and allows for brain penetration of [^{11}C]Loperamide. In both (**B**) and (**C**), the pituitary, a structure which exists outside the blood–brain barrier (BBB), is visible and shows uptake of [^{11}C]Loperamide.

Results

The *in-silico* assay of P-gp status identified 15 compounds that were more likely to be P-gp substrates and 21 that were more likely to undergo passive diffusion. The P-gp scores ranged from −3.46 to 1.02 and are listed in Table 1.

In-vitro equilibrium dialysis estimates in plasma and tissue are tabulated in Table 1. The plasma-free fraction estimates, f_P, ranged from 0.0012 to 0.63 (mean ± s.d.: 0.166 ± 0.163) and the tissue-free fraction, f_{ND}, ranged from 0.00069 to 0.55 (mean ± s.d.: 0.0767 ± 0.120). The free fraction ratio, f_P/f_{ND}, ranged from 0.090 to 25 (mean ± s.d.: 6.18 ± 5.74).

An example of the *in-vivo* PET image data for [^{11}C]Loperamide before and after inhibition of P-gp with cyclosporin-A (30 mg) is shown in Figure 1. The lack of brain penetration at baseline is clearly evident but high uptake ensues after inhibition of P-gp. In contrast, uptake in the pituitary, a structure that exists outside the BBB, is high and unaffected by P-gp modulation.

Plasma parent and whole blood input functions were successfully generated for all scans (Figure 2) with the metabolite data tending to be well described by an exponential approach to a constant (89% of compounds). Two-tissue compartment models were required for the majority of cerebellum TACs (78%) with the remaining well described by a one-tissue compartment model. The good quality of model fits for all compounds is evident from the results displayed in Figure 3 and the *in-vivo* PET parameter estimates derived from the kinetic analysis are tabulated in Table 1. The plasma to brain rate constant K_1 (mL/min/cm^3) ranged from 0.008 to 0.80 (mean ± s.d.: 0.309 ± 0.219) and the nondisplaceable equilibrium partition coefficient V_{ND} (mL/cm^3) ranged from 0.23 to 30 (mean ± s.d.: 5.17 ± 5.26).

The relationship between the equilibrium dialysis estimated free fraction ratio (f_P/f_{ND}) and the PET V_{ND} is displayed in Figure 4. In Figure 4, compounds which are predicted (*in-silico* assay) to be more likely to be P-gp substrates are depicted as solid circles and in Figure 4A many of these clearly fall below the line of identity which would indicate active efflux. In contrast, those compounds predicted to be more likely to undergo passive diffusion (open circles) are located around the line of identity. Furthermore, [^{11}C]Loperamide, a well-established P-gp substrate, falls well below the line of identity at baseline but returns near to it after P-gp inhibition (points joined by dashed line).

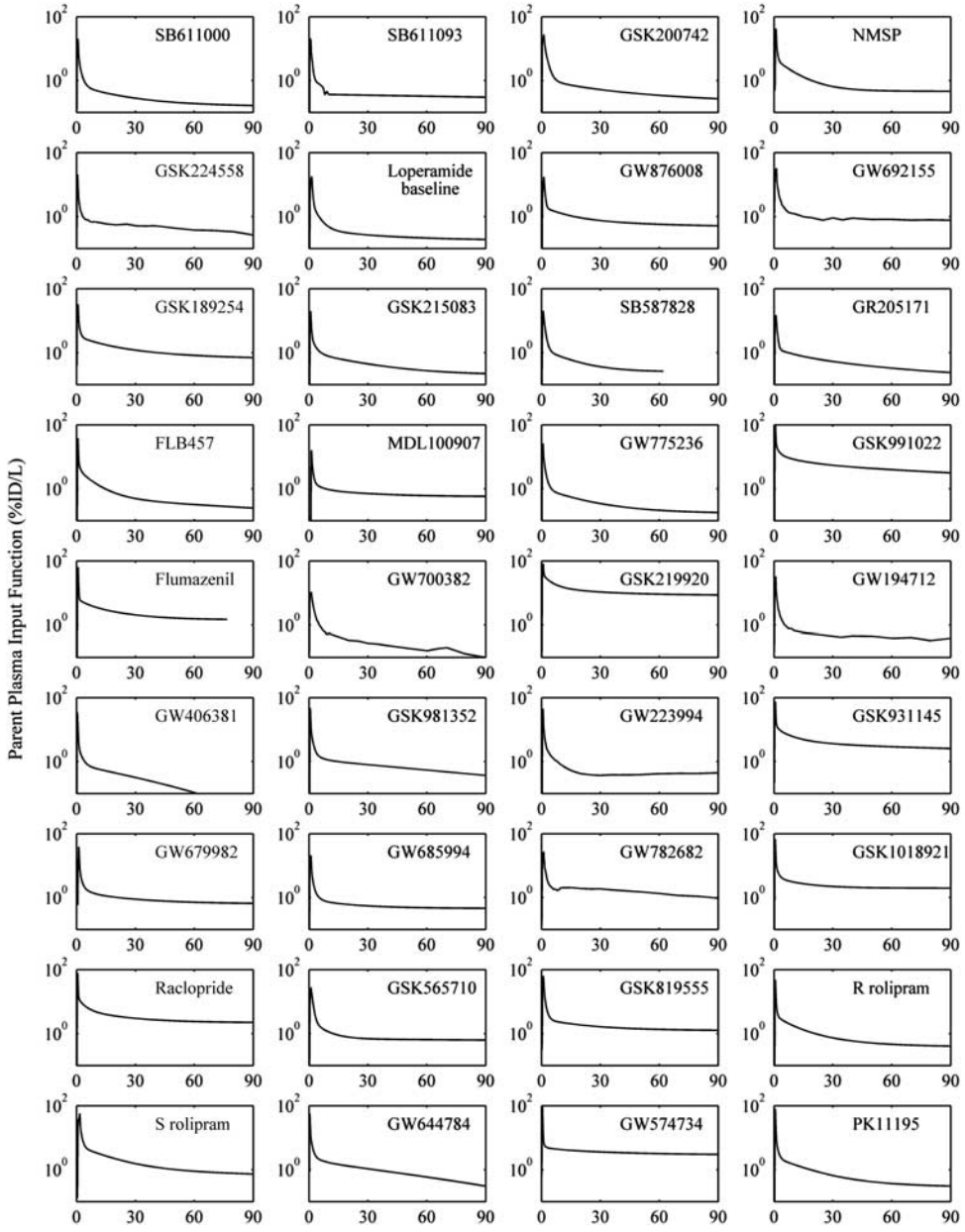

Figure 2 Positron emission tomography (PET) arterial plasma parent input functions for the ($n = 36$) radiolabelled compounds. For [^{11}C]Loperamide just the baseline input function is displayed.

To explore this further, the data were transformed into a Bland-Altman plot (Altman and Bland, 1983; Figure 4B) and the compounds predicted more likely to undergo passive diffusion were used to define 95% confidence intervals (dashed lines). Using these data, *Z*-tests were performed to classify compounds either as undergoing passive diffusion or active transport which resulted in 8 out of the 36 compounds being predicted as undergoing active efflux (SB-611000, SB-611093-AY, GSK200742, Loperamide, GW692155, SB-587828-A, GW775236, and GW223994). Of these, seven were predicted by the *in-silico* method to be likely P-gp substrates and the other one was near the borderline (GW223994: P-gp score = + 0.37). These classifications were also reflected in the K_1 values which were 0.11 ± 0.12 mL/min/cm^3 for the 8 compounds that the *Z*-test identified as P-gp substrates and 0.36 ± 0.21 mL/min/cm^3 for the other 28 compounds. These values were significantly different as determined from a two-sample *t*-test assuming unequal variance (t value = 4.29, df = 20 and $P < 0.0005$).

Discussion

We have combined quantitative PET studies of radiolabelled compounds to determine their total

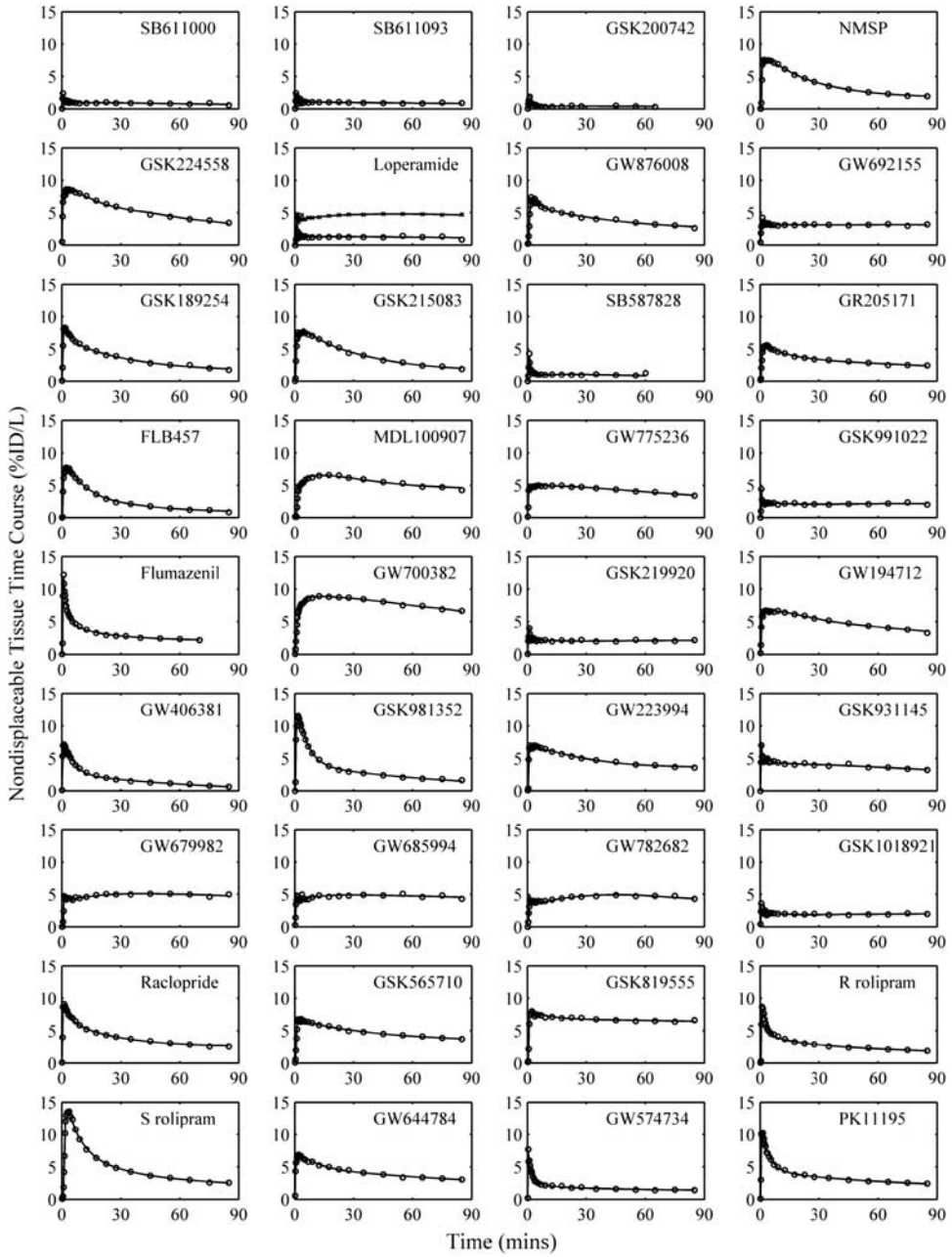

Figure 3 Positron emission tomography (PET) cerebellar time activity curves (TACs) for the ($n = 36$) radiolabelled compounds (○) and model fits from the parsimonious compartmental analysis (−). For [^{11}C]Loperamide two scans are shown, one at baseline (○) and the other after administration of 30 mg cyclosporin-A (×) which inhibits P-glycoprotein (P-gp).

in-vivo partition coefficient with *in-vitro* equilibrium dialysis assays of the free fractions in plasma and tissue to allow for a more comprehensive assay of BBB passage. Furthermore, the techniques that we have presented are applicable in humans and have direct relevance for human drug development strategies for CNS drugs. We explored the relationship between *in-vitro* equilibrium dialysis estimate of the partition coefficient (f_p/f_{ND}) and the *in-vivo* PET estimate of the partition coefficient in a region devoid of specific signal (V_{ND}) for 36 compounds in the Yorkshire-Landrace pig. To assess which of these compounds were likely to be P-gp substrates, we applied a proprietary *in-silico* prediction algorithm. For compounds that were predicted to enter the brain by passive diffusion there was good agreement between f_p/f_{ND} and V_{ND} as would be expected from theory. For about half the compounds that were predicted to be likely P-gp substrates V_{ND} was significantly lower than f_p/f_{ND}, again consistent with the theory for actively effluxed compounds. The other half was consistent with passive diffusion and it is hypothesized that this results from limitations of the *in-silico* modelling predictions of P-gp liability.

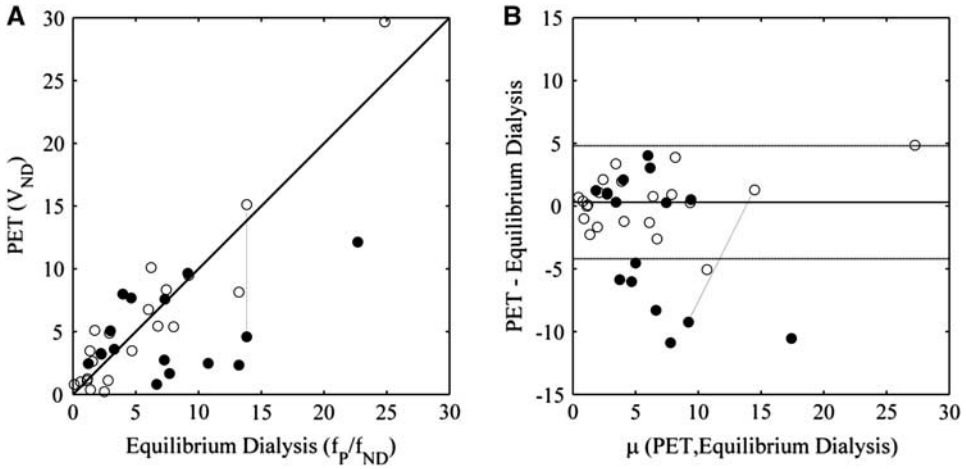

Figure 4 Comparison of *in-vitro* (equilibrium dialysis free fraction ratio—f_P/f_{ND}) and *in-vivo* (positron emission tomography (PET) nondisplaceable distribution volume—V_{ND}) measures. The symbols used indicate whether the *in-silico* modelling predicted that they were more likely to be P-glycoprotein (P-gp) substrates (●) or whether they were more likely to undergo passive diffusion (○). (**A**) Plot of equilibrium dialysis versus PET. (**B**) Bland-Altman plot of data in panel **A** using data from the compounds predicted *in-silico* to undergo passive diffusion (○) to define the confidence intervals (μ denotes the mean). In both plots, the data connected by the dashed line identify the results from the two [^{11}C]Loperamide scans (baseline (●) and the other after administration of 30 mg cyclosporin-A (○) which inhibits P-gp).

It is important to acknowledge that the major limitation of this work is likely to be the *in-silico* P-gp data. Future studies using MDCK cell lines or P-gp knockouts would be required to fully confirm this hypothesis. However, to further validate the approach, we examined two of the *in-vivo* experiments that were performed with Loperamide, which is a well-known P-gp substrate. On its own, tracer Loperamide produced a V_{ND} that was substantially lower than the measured f_p/f_{ND} and consistent with P-gp efflux, however, on repeating the PET experiment in the presence of cyclosporin-A (a known P-gp inhibitor) the V_{ND} estimate was in good agreement with f_p/f_{ND}. These data provided a strong validation of the theory. It should also be noted that we were only able to screen for P-gp liability and so we cannot rule out the involvement of other transport systems for some of these compounds. Although the fact that all major deviations from passive diffusion were identified by the P-gp screen may render this unlikely. It is important to emphasize that the methods presented do not allow for an explicit characterization of the transport process, i.e., they do not let us explicitly say that P-gp efflux is involved. Rather, the data that are obtained from the combined equilibrium dialysis and PET measures provide information relevant to the compound transport and facilitate estimation of the free brain concentration of the compounds under investigation.

While the limitations of the *in-silico* prediction of P-gp liability have already been discussed, there could also be errors associated with both the PET and equilibrium dialysis measurements. For the PET data, the presence of brain penetrant metabolites cannot be ruled out for all compounds. For the equilibrium dialysis data, the duration of dialysis, temperature and buffer conditions, and the fact that different pig brains were used for the *in-vitro* and *in-vivo* data could all introduce errors into the measurements. Although, the dialysis duration of 5 hours, used in this work, has been verified previously as appropriate for a range of GSK compound structures.

Two essential characteristics of a successful CNS drug are that it crosses the BBB and then interacts with the target at a pharmacologically active concentration. Measuring this in humans is important for derisking lead compounds and streamlining the drug development process. PET is ideally suited to measuring the BBB delivery of radiolabelled compounds in humans *in vivo*, but while it can determine the total brain to plasma partition coefficient, in isolation it cannot directly determine the free concentration in the tissue. Here, we have introduced the combination of PET with associated equilibrium dialysis measures of the free fraction in plasma and tissue that allow for the assessment of brain penetration, the transport process involved and measurement of the free concentration in tissue. The free tissue concentration in the brain can be calculated from the measurements as

$$C_{FT} = V_{ND}\frac{f_{ND}}{f_P}C_{FP} \qquad (13)$$

Further, by combining the estimate of the free brain concentration of the drug with an *in-vitro* estimate of the affinity for its target (K_D), it is possible to obtain an estimate of the target occupancy.

$$Occ = \frac{C_{FT}}{C_{FT} + K_D} \qquad (14)$$

The resultant accuracy of such occupancy predictions is dependent on whether the *in-vitro* K_D truly

reflects the *in-vivo* K_D. Some care should be taken here as there is evidence that *in-vitro* assay conditions such as the temperature and the buffer used are important (Laruelle *et al*, 1994) in addition to *in-vitro–in-vivo* differences in the tissue environment which adds a degree of uncertainty to this prediction of target occupancy.

The measurement of free fractions in plasma and tissue with equilibrium dialysis may have additional important advantages for the PET field. For instance, Guo *et al* (2009) have already used these assays in biomathematical tools to aid radiotracer discovery programs where they add particular value in helping to account for nonspecific binding. In addition, plasma-free fraction estimates are used in quantitative studies comparing binding potentials between groups of individuals where nonspecific binding may be different. It may be that equilibrium dialysis measures offer a more accurate assay over ultrafiltration methods used previously, particularly for highly protein bound compounds (Adams *et al*, 2004) and future studies will be needed to assess this in more detail.

In summary, equilibrium dialysis measures of the free fraction in plasma and tissue are valuable in aiding the interpretation of *in-vivo* PET data. While the focus of this paper has been on using them to assess free drug concentrations in the CNS, they could also have a significant role in radiotracer discovery and accurate quantification of receptor binding.

Acknowledgements

The authors would like to thank Jan Passchier, Tom Bonasera, and Idriss Bennacef for help sourcing compounds; Ann Hersey for help and discussions around the *in-silico* P-gp prediction; Alberto Ruffo and Alexander Stevens for help with the equilibrium dialysis assays; Ilan Rabiner for interesting discussions; and the Aarhus PET centre staff for helping in the acquisition of all the *in-vivo* PET data over a number of years of excellent collaboration.

Disclosure/conflict of interest

All employees of GlaxoSmithKline are identified by their affiliations.

References

Abi-Dargham A, Simpson N, Kegeles L, Parsey R, Hwang DR, Anjilvel S, Zea-Ponce Y, Lombardo I, Van HR, Mann JJ, Foged C, Halldin C, Laruelle M (1999) PET studies of binding competition between endogenous dopamine and the D1 radiotracer [11C]NNC 756. *Synapse* 32: 93–109

Adams KH, Pinborg LH, Svarer C, Hasselbalch SG, Holm S, Haugbøl S, Madsen K, Frøkjær V, Martiny L, Paulson OB, Knudsen GM (2004) A database of [18F]-altanserin binding to 5-HT2A receptors in normal volunteers: normative data and relationship to physiological and demographic variables. *Neuroimage* 21:1105–13

Altman DG, Bland JM (1983) Measurement in medicine: the analysis of method comparison studies. *Statistician* 32:307–17

Borst P, Oude Elferink R (2002) Mammalian ABC transporters in health and disease. *Annu Rev Biochem* 71: 537–92

Cordon-Cardo C, O'Brien JP, Casals D, Rittman-Grauer L, Biedler JL, Melamed MR, Bertino JR (1989) Multidrug-resistance gene (P-glycoprotein) is expressed by endothelial cells at blood-brain barrier sites. *Proc Natl Acad Sci USA* 86:695–8

Cunningham VJ, Parker CA, Rabiner EA, Gee AD, Gunn RN (2005) PET studies in drug development: methodological considerations. *Drug Discov Today* 2:311–5

Gandelman MS, Baldwin RM, Zoghbi SS, Zea-Ponce Y, Innis RB (1994) Evaluation of ultrafiltration for the free-fraction determination of single photon emission computed tomography (SPECT) radiotracers: beta-CIT, IBF, and iomazenil. *J Pharm Sci* 83:1014–9

Giacomini KM, Huang S-M, Tweedie DJ, Benet LZ, Brouwer KLR, Chu X, Dahlin A, Evers R, Fischer V, Hillgren KM, Hoffmaster KA, Ishikawa T, Keppler D, Kim RB, Lee CA, Niemi M, Polli JW, Sugiyama Y, Swaan PW, Ware JA, Wright SH, Wah Yee S, Zamek-Gliszczynski MJ, Zhang L (2010) Membrane transporters in drug development. *Nat Rev Drug Discov* 9:215–36

Guo G, Brady M, Gunn RN (2009) A biomathematical modeling approach to central nervous system radioligand discovery and development. *J Nucl Med* 50: 1715–23

Hammarlund-Udenaes M, Bredberg U, Fridén M (2009) Methodologies to assess brain drug delivery in lead optimization. *Curr Top Med Chem* 9:148–62

Hammarlund-Udenaes M, Fridén M, Syvänen S, Gupta A (2008) On the rate and extent of drug delivery to the brain. *Pharm Res* 25:1737–50

Innis RB, Cunningham VJ, Delforge J, Fujita M, Gjedde A, Gunn RN, Holden J, Houle S, Huang SC, Ichise M, Iida H, Ito H, Kimura Y, Koeppe RA, Knudsen GM, Knuuti J, Lammertsma AA, Laruelle M, Logan J, Maguire RP, Mintun MA, Morris ED, Parsey R, Price JC, Slifstein M, Sossi V, Suhara T, Votaw JR, Wong DF, Carson RE (2007) Consensus nomenclature for *in vivo* imaging of reversibly binding radioligands. *J Cereb Blood Flow Metab* 27:1533–9

Jeffrey P, Summerfield SG (2007) Challenges for blood-brain barrier (BBB) screening. *Xenobiotica* 37:1135–51

Kalvass JC, Maurer TS (2002) Influence of nonspecific brain and plasma binding on CNS exposure: implications for rational drug discovery. *Biopharm Drug Dispos* 23:327–38

Kinahan PE, Rogers JG (1989) Analytic 3D image-reconstruction using all detected events. *IEEE Trans Nucl Sci* 36:964–8

Laruelle M, Giddings SS, Zea-Ponce Y, Charney DS, Neumeyer JL, Baldwin RM, Innis RB (1994) Methyl 3β-(4-[125I]iodophenyl)tropane-2β-carboxylate *in vitro* binding to dopamine and serotonin transporters under 'physiological' conditions. *J Neurochem* 62:978–86

Qadir M, O'Loughlin KL, Fricke SM, Williamson NA, Greco WR, Minderman H, Baer MR (2005) Cyclosporin A is a broad-spectrum multidrug resistance modulator. *Clin Cancer Res* 11:2320–6

Read KD, Braggio S (2010) Assessing brain free fraction in early drug discovery. *Expert Opin Drug Metab Toxicol* 6:337–44

Summerfield SG, Stevens AJ, Cutler L, del Carmen OM, Hammond B, Tang SP, Hersey A, Spalding DJ, Jeffrey P (2006) Improving the *in vitro* prediction of *in vivo* central nervous system penetration: integrating permeability, P-glycoprotein efflux, and free fractions in blood and brain. *J Pharmacol Exp Ther* 316:1282–90

Wienhard K, Dahlbom M, Eriksson L, Michel C, Bruckbauer T, Pietrzyk U, Heiss WD (1994) The ECAT EXACT HR: performance of a new high resolution positron scanner. *J Comput Assist Tomogr* 18:110–8